IJBPAS, July, 2015, 4(7): 4912-4924

ISSN: 2277–4998

International Journal of Biology, Pharmacy and Allied Sciences (IJBPAS)

'A Bridge Between Laboratory and Reader'

www.ijbpas.com

NANOHYDROXYAPATITE PRODUCTION BY BIOFILM OF *SERRATIA MARCESCENS* AND *PSEUDOMONAS AERUGINOSA* IN POLYURETHANE FOAM

TAYEBEH AKBARI[1], ANITA KHANAFARI [1], MOAHMOUD REZA SOHRABI[2]

[1.] Faculty of Bioscience, Islamic Azad University, North Tehran Branch, Pasdaran, Tehran- Iran

[2.] Faculty of Chemistry, Islamic Azad University, North Tehran Branch, Pasdaran, Tehran- Iran

ABSTRACT

Hydroxyapatite (HA) has been used as an important material in biomedical applications, bone substitute and implant coatings due to its high similarity to inorganic components in bone and tooth structures. In this study, production of nano-hydroxyapatite biomineralization was investigated. To produce nano-hydroxyapatite, bacterial strains, *Pseudomonas aeruginosa* PTCC1670 and *Serratia marcescens* ATCC 14756 were grown as biofilms on a polyurethane substrates. The microorganisms are able to produce extracellular crystals of HA by enzymatic cleavage of ß-glycerophosphate in the presence of calcium chloride. After the growth of bacteria on polyurethane foam, biomineralisation and subsequent sintering, three-dimensional HA scaffold was formed. The results showed that the bacterial's biofilms of *Serratia marcescens* and *Pseudomonas aeruginosa* on polyurethane foam produced 0.482 g/L and 0.779 g/L HA powder respectively. The properties of the resulting powders were evaluated by using X-ray diffraction (XRD), Fourier Transform Infra-Red Spectroscopy (FTIR) and scanning electron microscopy (SEM). HA size distribution data obtained by SEM is 25-55 nm and 20-37 nm for *Serratia* and *Pseudomonas*, respectively.

Keywords: NanoHydroxyapatite; Microbial mineralization*; Pseudomonas aeruginosa*; *Serratia marcescens*; polyurethane foam; Nanocomposite

INTRODUCTION

Hydroxyapatite (HA) is one of the most prominent biominerals in primary naturally hard tissues (Rajkumar et al., 2011a). This material has been significantly more interested because of similarity to natural calcium phosphate presents in biological hard tissue (Balamurugan et al., 2005a). HA ceramics that belonged to a class of phosphate-based materials have been widely used in bone substitute materials, implants (Sanosh et al., 2009a) and dental materials (Nayak, 2010a; Rajkumar et al., 2011b; Ramli et al., 2011a).

Bone is a dynamic and highly vascularized tissue with a unique capacity to heal and remodel without leaving a scar. It is the structural framework of the body and is composed of an inorganic mineral phase of hydroxyapatite and an organic phase of mainly type I collagen (Martins et al., 2009a). For bone repairing or replacement, the selected material must be able to make bond with host living bones. HA form a chemical bond with the host tissue and its porous character offers high binding affinity for biological substances such as enzymes, hormones, antibiotics, antibody fragments, steroids, etc. Also, synthetic Hydroxyapatite based materials is thermodynamically stable at physiological pH and osteoconductive provided that fully differentiated osteogenic cells are available at the site of implantation (Beganskienė et al., 2006a; Martins et al., 2009b; Nayak, 2010b).

Bone mineral crystals are usually nano-sized. Calcium phosphate presence in bone is in the form of nano-sized needlelike crystals of nearly 5-20 nm width and 60 nm lengths, with an inconsiderable crystallized nonstoichiometric apatite phase containing CO^{2-}, Na^{+}, F^{-} and other ions in a collagen fiber matrix (Balamurugan et al., 2005b). Thus, engineering HA at nano-scale would have greater functional properties due to its large surface area, small grain size and similarity to biological apatite, which would have a greater effect on implant-cell interaction in human body (Ramakrishna et al., 2001; Sanosh et al., 2009b). Moreover, Ca^{2+} ions release from the nano HA powders were found to be similar to bone apatite and significantly faster than microscale sized counterpart. So, nano HA powders can be utilized as biomaterials due to the excellent biocompatibility and bioactivity (V. Dorozhkin, 2012a).

Because of abundant applications of HA in biomedical structures, scientific community

research about new methodologies for HA synthesis with optimum properties closer to those of living hard tissues like bone and teeth , intend to improve biomedical applications (Nayak, 2010b; Ramli et al., 2011b). These methods include precipitation (Nayak, 2010b), hydrothermal (Agrawal et al., 2011a; Beganskienė et al., 2006b), mechanochemical (Adzila et al., 2011; Agrawal et al., 2011b), sol–gel (Agrawal et al., 2011b; Balamurugan et al., 2005b; Chai and Ben-Nissan, 1999), biomimetic deposition (Cüneyt Tas, 2000; Hutchens et al., 2006; Thamaraiselvi et al., 2006), biomineralization (Macaskie et al., 2005; Mostaghaci et al., 2009). Biomineralization is controlled crystallisation of an inorganic phase, often via the extracellular polymeric matrix (EPM) of biomass, in which inorganic crystals can be assembled (Mann, 1993).

Present study deals with new HA formulation and bioproduction of this material with properties closer to the bone include nanosized and monolithic structures by two standard bacteria *Serratia marcescens* and *Pseudomonas aeruginosa*. Microorganisms can be pre-grown as a biofilm on the surfaces of various support materials (Macaskie et al., 2000; Thackray et al., 2004). The cells generate phosphate precipitant enzymatically using phosphatase'tethered' within the (EPM) (Macaskie et al. 2000). Therefore, this could impart a non line-of-sight threedimensional (3D) patterning with calcium phosphate biomineral encrusted on the surface of the biofilm. At final, organic supporting layer and the biofilm matrix can be removed by sintering to leave a HA skeleton (Kim et al., 2008; Macaskie et al., 2005b). The second object of this study is to compare the HA nanoparticle production potential of *P. aeruginosa* with *S. marcescens* to introduce a new possible candidate to biomimetic synthesize of HA nanoparticles.

Material and methods

2.1. Bacterial strains in used:

Two standard bacterial strains, *Pseudomonas aeruginosa* PTCC 1570 and *Serratia marcescens* ATCC 14756 were prepared from Iran Scientific and Industrial Research Organization Pasteur Institute of Iran, respectively. The purity of each bacteria was affirmed by standard biochemical tests (according to Khanafari et al, 1998 (Khanafari and Hosseini, 2012)).

2.2. Bacterial inocula culture:

Cultures were grown in shaking incubators at 27 °C and 120 rpm for 24-48 h in capped 250 ml Erlenmeyer flasks containing nutrient broth medium (Merck, Germany). Bacterial cell density was adjusted on 0.08-0.1 at 600 nm by UV-VIS scanning spectrophotometer, UV 2101 pc, Shimadzu (31).

2.2. Preparation n-HA powder

At first step, the polyurethane foam was shredded in 2×2×4 cm cubes as a bed of biofilm production, and were hanged in two Erlenmeyer flasks (12 cubes per each Erlenmeyer flasks) containing 1600 ml NB medium. Then NB medium containing polyurethane foam cubes were autoclaved at 121 °C for 15 min. After cooling to room temperature, NB medium containing polyurethane foam cubes inoculated with 160 ml inocula culture of each bacteria and were incubated at 32-35 °C. After about one month, the exterior surface of foam cubes was observed by the loop microscope to confirm the growth of each bacteria as a biofilm on polyurethane foams. Foam cubes were transferred to mineral medium, which were prepared by 25 mM calcium chloride (Sigma, USA) and 50 mM B-Glycerophosphate disodium salt hydrate (Sigma, USA) were used as calcium and phosphorus donors, at pH 8.6 and were incubated at 32-35 °C for 14 days. Then, the cubes were dislodged from mineral medium and air dried in oven at 60°C for 12 hours. They were sintered in a furnace for two hours at 600 °C to produce a solid scaffold. Dried foam cubes were pounded and crushed to obtain the crystalline powder and analysed to discriminate HA powder production ability of two mentioned bacteria according to Sammons et al., 2007.

2.3. Loop microscopy

Loop microscopy study was performed by (STMPRO-B, Italy) instrument to determine bacterial growth and transfiguration on foam cubes.

2.4. X-ray Diffractometry analysis

The crystal structure and the content phase present in obtaining samples were examined with X-ray diffraction (XRD) by (PANalitical, X PERTPRO) instrument. The crystallite size of the obtained powders was calculated from the XRD data by using the Scherrer equation. That is, $D = 0.9k/b\cos h$, where D is the average crystallite size, b is the full width was measured at half-maximum of the HA, k is the wavelength of X-rays (0.154 nm), and h is the peak

diffraction angle (Nikpour et al., 2012).

2.5. Fourier Transform Infra-Red Spectroscopy (FTIR)

The structure of obtaining powders was approved by FTIR spectrum. These samples were analyzed by FTIR analysis (ASTM D3677, Germany) spectrometer within scanning range of 400-4000 cm-1. The FTIR spectroscopy has provided quality information about the structure of HA powder and this test was used to perceive the characteristic peaks of product.

2.6. Electron Microscopy analysis

This test carried out by Scanning electron microscopy (EM3200, KYKY China) tocharacterize the morphology and nanoparticle size. The samples put up on aluminum stand be were supported and were coating with gold thin film fore better conductivity.

RESULTS

3.1. Loop analysis:

Trough observing the surface of foam cubes by Loop microscope, the exterior surface of cubes were withdrawn from each medium including 10% inocula culture of each bacteria was crinkly and glossy with yellowish complexion.

3.2. XRD analysis:

In XRD patterns of prepared powders of bacteria: *S. marcescense* and *Ps. aeroginosa*, presence of a small remnants of sodium chloride and other phosphate salt impurity (approximately 1%) was indicated. Presence of Sodium ions within samples may not be unfavorable clinical effects because of presenting approximately 1% Sodium in bone structure (Sammons et al., 2007b). These XRD patterns are shown in (fig. 2 and 3), respectively. The high intensity and wide breadth of the peaks demonstrate that the particles are highly crystalline and nano scale size. The average crystallite size that estimated by using the Scherrer equation for the n-HA from *S. marcescens* and *Ps. aeruginosa* were 65.1 and 36.4 nm, respectively.

3.3. FTIR analysis:

The FT-IR spectra of samples obtained by *S.marcescens* and *Ps. aeruginosa* are shown in (Fig. 4 and 5), respectively. The peak at (1104-1043cm^{-1}), (572-596 cm^{-1}) and (470-471cm^{-1}) regions indicate P-O band in a PO_4^{-2} and P-O-P band in PO_4^{-3} groups (Rajkumar et al., 2011b). The peak at (860-877cm^{-1}) region indicates P-O-H band in HPO_4^{-} and the peak at (2600-3500 cm^{-1})

regions indicates O-H bands which all of these bands confirm the presence of HA phase in both samples (Sammons et al., 2007b).

3.4. SEM analysis:

SEM images of nanoHA powders produced by S. *marcescens* and *Ps. aeruginosa* are shown in fig. 6 and fig. 7 respectively. The SEM image of powders produced by both bacteria showed spherical and cylindrical particles, most spherical, between 20-37 nm. Particles had the homogeneous distribution.

Fig 1: SEM image loop of polyurethane foam. a) Foam cubes before bacterial growth b) Foam cubes that has been in NB medium for 1 month c) figure b with 10X magnifications.

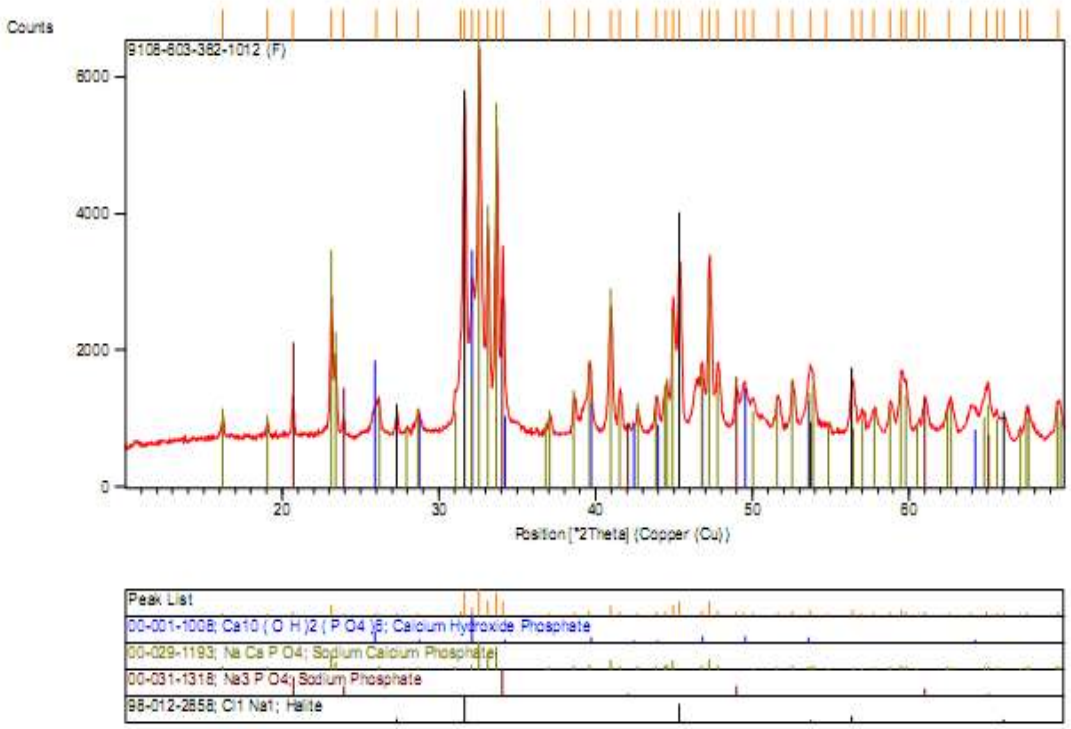

Fig. 2- The XRD pattern of HA produced by *S. marcescens*

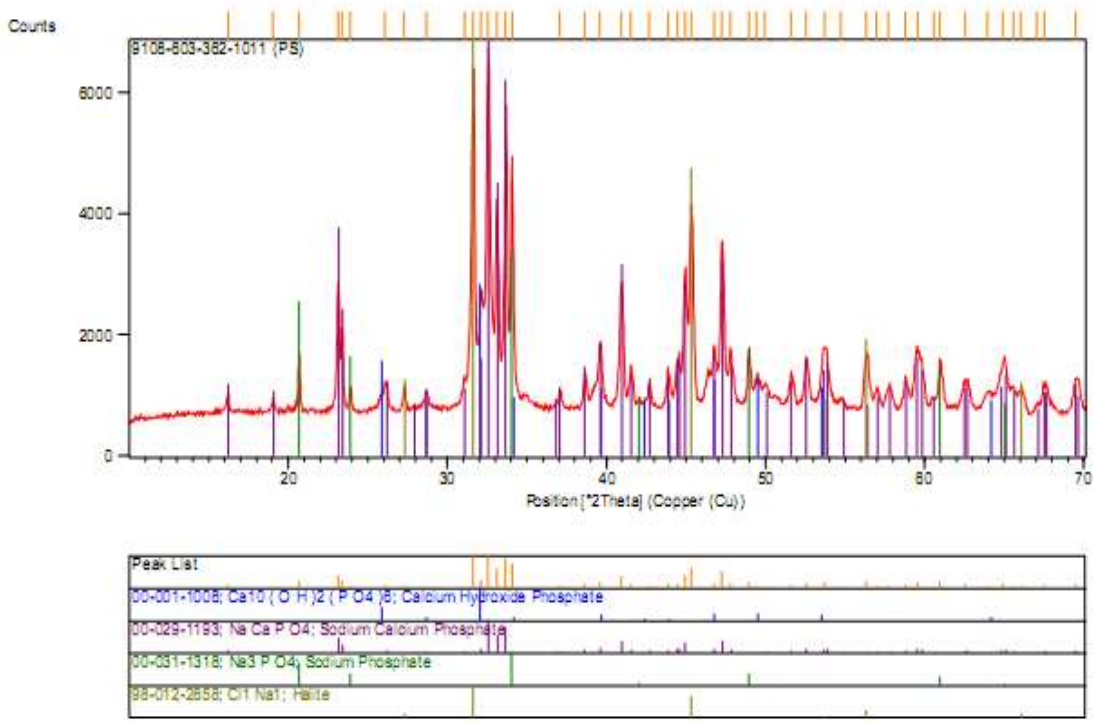

Fig. 3- The XRD pattern of HA produced by *Ps. Aeruginosa*

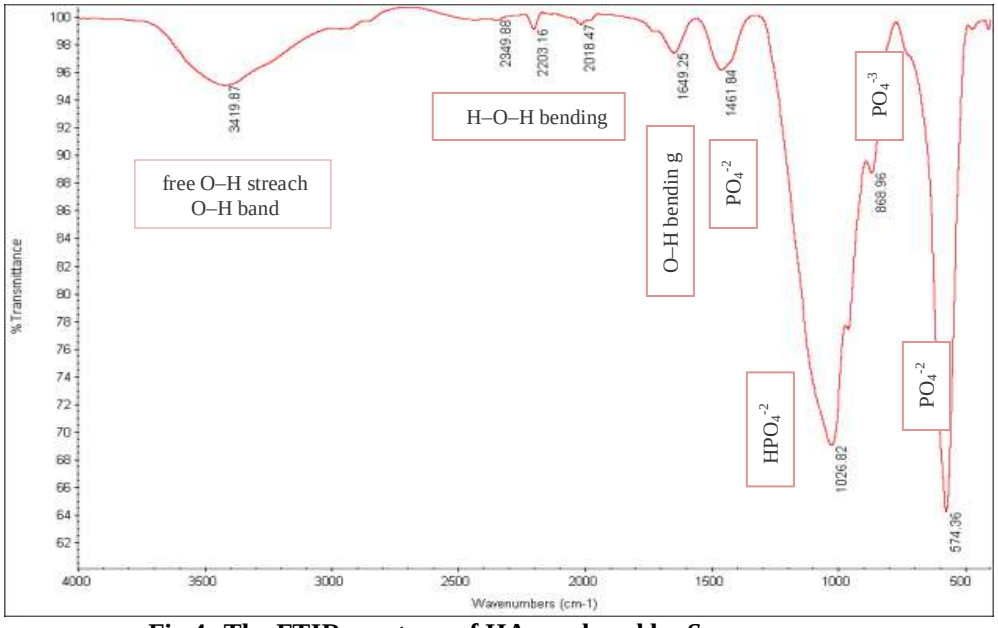

Fig.4- The FTIR spectrumof HA produced by *S. marcescens*

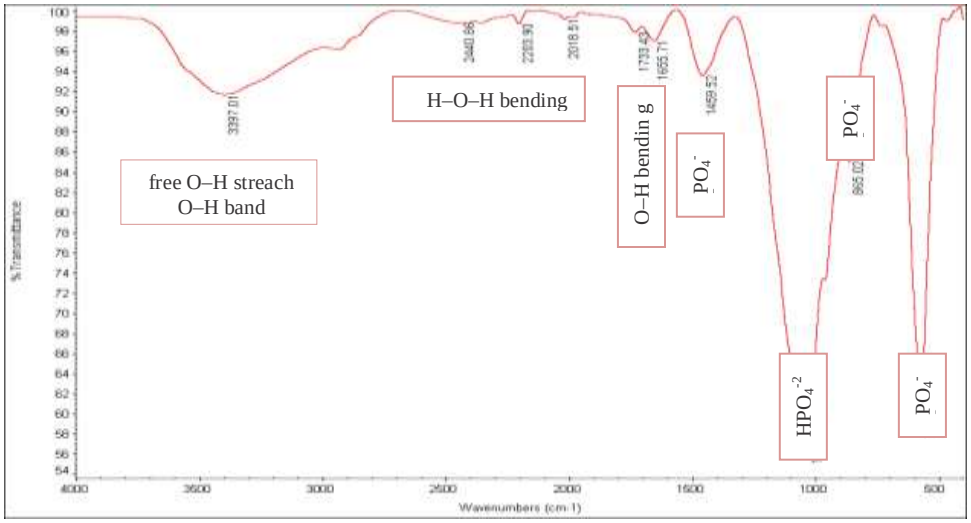

Fig.5- The FTIR spectrumof HA produced by *Ps. aeruginosa*

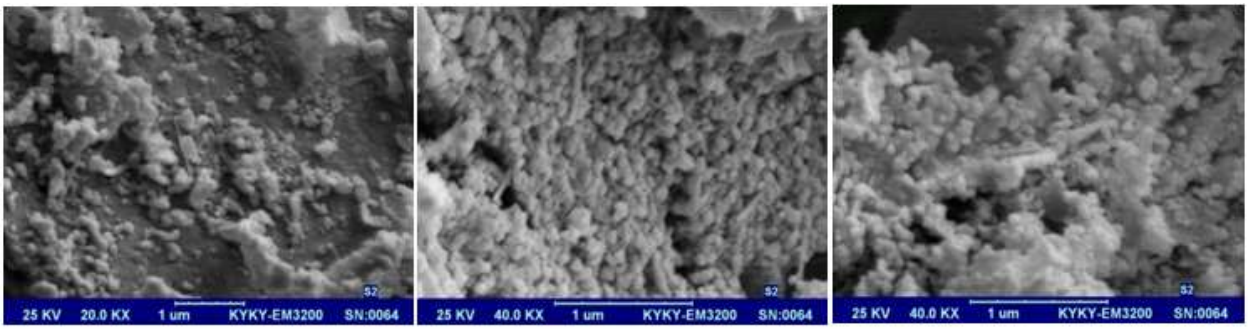

Fig. 6- The SEM images of HA produced by *S. marcescens* with 20.0 and 40.0 KX magnifications.

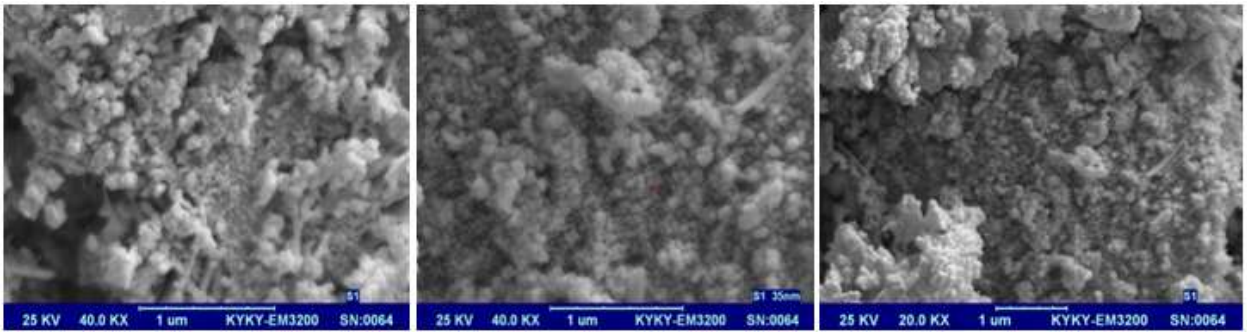

Fig. 7- The SEM images of HA produced by *Ps. aeruginosa* with 20.0 and 40.0 KX magnification.

DISCUSSION

Hydroxyapatite has some properties such as biocompatibility, bioactivity and biodegradability which are under the optimum level when this material was produced in nano scale and the uniform distribution (Mittal et al., 2010; Nayak, 2010b; Santos et al., 2004). The current work attempted to study a methodology for HA synthesis with optimum properties closer to those of living hard tissues like bone and teeth, intend by better and more effective biomedical applications.

According to the results of this research and before studies, it seems chemical methods such as Sol-gel need more control on lab variables and repeated examination to reach to optimum properties of the product than the applied procedure in our experiment (Ferraz et al., 2004; Meyers et al., 2008; V. Dorozhkin, 2012b). Beside, this work as the first report on using of *Ps. aeruginosa* to produce HA nanopowders by biomineralization, demonstrated that *Ps. aeruginosa* produce HA particles (0.779 g/L) in higher concentration than *S. marcescens* (0.482 g/L), so it may be a suitable producer of HA particles in comparing with *S. marcescens.* Also, size and size distribution of nanoparticles produced by *Ps. aeruginosa* showed good result when compared with similar works while nanoparticles produced by *S. marcescens* did not show significant difference with before studies (Macaskie et al., 2005b; Mostaghaci et al., 2009b; Sammons et al., 2007b; Yong et al., 2004).

CONCLUSION

As was confirmed the next statement, the usage of bacteria in producing HA is a non-toxic and cheap procedure with most simulated structure to natural bone. The biomineralized HA nano powders meet demanded properties for dental and orthopedics applications. The materials was identified by X-ray powder diffraction analysis, and the size of crystallites was measured as 25-50 nm and 20-37 nm for *S. marcescens* and *Ps. aeruginosa*, respectively. Because of tiny size of obtained particles in nano scale, they are suitable candidate for using in vivo as biosensors and drug delivery systems.

REFERENCES

[1] Adzila, S., Sopyan, I., Hamdi, M., 2011. Synthesis of Hydroxyapatite through Dry Mechanochemical Method and Its Conversion to Dense Bodies : Preliminary Result 97–101.

[2] Agrawal, K., Singh, G., Puri, D., Prakash, S., 2011a. Synthesis and Characterization of Hydroxyapatite Powder by Sol-Gel Method for Biomedical Application 10, 727–734.

[3] Agrawal, K., Singh, G., Puri, D., Prakash, S., 2011b. Synthesis and Characterization of Hydroxyapatite Powder by Sol-Gel Method for Biomedical Application 10, 727–734.

[4] Balamurugan, A., Michel, J., Faure, J., Benhayoune, H., Wortham, L., Sockalingum, G., Banchet, V., Bouthors, S., Laurent-Maquin, D., Balossier, G., 2005a. SYNTHESIS

AND STRUCTURAL ANALYSIS OF SOL GEL DERIVED. Ceramics 27–31.

[5] Balamurugan, A., Michel, J., Faure, J., Benhayoune, H., Wortham, L., Sockalingum, G., Banchet, V., Bouthors, S., Laurent-Maquin, D., Balossier, G., 2005b. SYNTHESIS AND STRUCTURAL ANALYSIS OF SOL GEL DERIVED. Ceramics 27–31.

[6] Beganskienė, A., Dudko, O., Sirutkaitis, R., Giraitis, R., 2006a. Water Based Sol-Gel Synthesis of Hydroxyapatite 9, 4–7.

[7] Beganskienė, A., Dudko, O., Sirutkaitis, R., Giraitis, R., 2006b. Water Based Sol-Gel Synthesis of Hydroxyapatite 9, 4–7.

[8] Chai, C.S., Ben-Nissan, B., 1999. Bioactive nanocrystalline sol-gel hydroxyapatite coatings. J. Mater. Sci. Mater. Med. 10, 465–469.

[9] Cüneyt Tas, A., 2000. Synthesis of biomimetic Ca-hydroxyapatite powders at 37°C in synthetic body fluids. Biomaterials 21, 1429–1438.

[10] Ferraz, M.P., Monteiro, F.J., Manuel, C.M., 2004. Hydroxyapatite nanoparticles : A review of 74–80.

[11] Hutchens, S.A., Benson, R.S., Evans, B.R., Neill, H.M.O., Rawn, C.J., 2006. Biomimetic synthesis of calcium-deficient hydroxyapatite in a natural hydrogel 27, 4661–4670.

[12] Khanafari, A., Hosseini, F., 2012. Practical Microbiology with Biochemic al Function and Colord Atlas. Poorsina Publ. 22, 279–287.

[13] Kim, Y.J., Lee, Y.H., Lee, M.H., Kim, H.J., Pan, J.H., Lim, G. Il, Choi, Y.S., Kim, K., Park, N., Lee, C., Lee, W.I., 2008. Formation of Efficient Dye-Sensitized Solar Cells by Introducing an Interfacial Layer of Long-Range Ordered Mesoporous TiO 2 Thin Film 13225–13230.

[14] Macaskie, L.E., Bonthrone, K.M., Yong, P., Goddard, D.T., 2000. Enzymically mediated bioprecipitation of uranium by a Citrobacter sp. : a concerted role for exocellular lipopolysaccharide and associated phosphatase in biomineral formation. Microbiology 146 (Pt 8, 1855–67.

[15] Macaskie, L.E., Yong, P., Paterson-Beedle, M., Thackray, A.C., Marquis, P.M., Sammons, R.L., Nott, K.P., Hall, L.D., 2005a. A novel non line-

of-sight method for coating hydroxyapatite onto the surfaces of support materials by biomineralization. J. Biotechnol. 118, 187–200.

[16] Macaskie, L.E., Yong, P., Paterson-Beedle, M., Thackray, A.C., Marquis, P.M., Sammons, R.L., Nott, K.P., Hall, L.D., 2005b. A novel non line-of-sight method for coating hydroxyapatite onto the surfaces of support materials by biomineralization. J. Biotechnol. 118, 187–200.

[17] Mann, S., 1993. Molecular tectonics in biomineralization and biomimetic materials chemistry. Nature 365, 499–505.

[18] Martins, A.M., Alves, C.M., Reis, R.L., Mikos, A.G., Kasper, Kurtis, F., 2009a. Toward Osteogenic Differentiation of Marrow Stromal Cells and In Vitro Production of Mineralized Extracellular Matrix onto Natural Scaffolds, in: Puleo, D.A., Bizios, R. (Eds.), Springer US, New York, NY, pp. 1–20.

[19] Martins, A.M., Alves, C.M., Reis, R.L., Mikos, A.G., Kasper, Kurtis, F., 2009b. Toward Osteogenic Differentiation of Marrow Stromal Cells and In Vitro Production of Mineralized Extracellular Matrix onto Natural Scaffolds, in: Puleo, D.A., Bizios, R. (Eds.), Springer US, New York, NY, pp. 1–20.

[20] Meyers, M.A., Chen, P.-Y., Lin, A.Y.-M., Seki, Y., 2008. Biological materials : Structure and mechanical properties. Prog. Mater. Sci. 53, 1–206.

[21] Mittal, M., Prakash, S., Nath, S.K., Sapra, P.K., 2010. PREPARATION METHODOLOGY of HYDROXYAPATITE POWDER : A REVIEW Hydrolysis of Brushite by 4 . Preparation of HAP by the Combustion Method from Egg Shell 378–381.

[22] Mostaghaci, B., Fathi, M.H., Sheikh Zeinoddin, M., Soleimanian Zad, S., 2009a. Bacterial synthesis of nanostructured hydroxyapatite using - GetInfo [WWW Document]. Inderscience Enterp. URL https://getinfo.de/app/Bacterial-synthesis-of-nanostructured-hydroxyapatite/id/BLCP:CN073637087 (accessed 7.11.13).

[23] Mostaghaci, B., Fathi, M.H., Sheikh Zeinoddin, M., Soleimanian Zad, S., 2009b. Bacterial synthesis of nanostructured hydroxyapatite using - GetInfo [WWW Document]. Inderscience Enterp.

[24] Nayak, A.K., 2010a. Hydroxyapatite Synthesis Methodologies : An Overview 2, 903–907.

[25] Nayak, A.K., 2010b. Hydroxyapatite Synthesis Methodologies : An Overview 2, 903–907.

[26] Nikpour, M.R., Rabiee, S.M., Jahanshahi, M., 2012. Synthesis and characterization of hydroxyapatite/chitosan nanocomposite materials for medical engineering applications. Compos. Part B Eng. 43, 1881–1886.

[27] Rajkumar, M., Meenakshisundaram, N., Rajendran, V., 2011a. Development of nanocomposites based on hydroxyapatite/sodium alginate: Synthesis and characterisation. Mater. Charact. 62, 469–479.

[28] Rajkumar, M., Meenakshisundaram, N., Rajendran, V., 2011b. Development of nanocomposites based on hydroxyapatite/sodium alginate: Synthesis and characterisation. Mater. Charact. 62, 469–479.

[29] Ramakrishna, S., Mayer, J., Wintermantel, E., Leong, K.W., 2001. Biomedical applications of polymer-composite materials : a review 61.

[30] Ramli, R.A., Adnan, R., Bakar, M.A., 2011a. Synthesis and Characterisation of Pure Nanoporous Hydroxyapatite 22, 25–37.

[31] Ramli, R.A., Adnan, R., Bakar, M.A., 2011b. Synthesis and Characterisation of Pure Nanoporous Hydroxyapatite 22, 25–37.

[32] Sammons, R., Thackray, a C., Ledo, H.M., Marquis, P.M., Jones, I.P., Yong, P., Macaskie, L.E., 2007a. Characterisation and sintering of nanophase hydroxyapatite synthesised by a species of Serratia. J. Phys. Conf. Ser. 93, 012048.

[33] Sammons, R., Thackray, a C., Ledo, H.M., Marquis, P.M., Jones, I.P., Yong, P., Macaskie, L.E., 2007b. Characterisation and sintering of nanophase hydroxyapatite synthesised by a species of Serratia. J. Phys. Conf. Ser. 93, 012048.

[34] Sanosh, K.P., Chu, M.-C., Balakrishnan, a., Kim, T.N., Cho, S.-J., 2009a. Preparation and characterization of nano-hydroxyapatite powder using sol-gel technique. Bull. Mater. Sci. 32, 465–470.

[35] Sanosh, K.P., Chu, M.-C., Balakrishnan, a., Kim, T.N., Cho, S.-J., 2009b. Preparation and characterization of nano-hydroxyapatite powder using sol-gel technique. Bull. Mater. Sci. 32, 465–470.

[36] Santos, M.H., Oliveira, M. De, Souza, L.P.D.F., Mansur, H.S., Vasconcelos, W.L., 2004. Synthesis control and characterization of hydroxyapatite prepared by wet precipitation process. Mater. Res. 7, 625–630.

[37] Thackray, A.C., Sammons, R.L., Macaskie, L.E., Yong, P., Lugg, H., Marquis, P.M., 2004. Bacterial biosynthesis of a calcium phosphate bone-substitute material. J. Mater. Sci. Mater. Med. 15, 403–6.

[38] Thamaraiselvi, T. V, Prabakaran, K., Rajeswari, S., 2006. Synthesis of Hydroxyapatite that Mimic Bone Minerology 19, 81–83.

[39] V. Dorozhkin, S., 2012a. Nanodimensional and Nanocrystalline Calcium Orthophosphates. Am. J. Biomed. Eng. 2, 48–97.

[40] V. Dorozhkin, S., 2012b. Nanodimensional and Nanocrystalline Calcium Orthophosphates. Am. J. Biomed. Eng. 2, 48–97.

[41] Yong, P., Macaskie, L.E., Sammons, R.L., Marquis, P.M., 2004. Synthesis of nanophase hydroxyapatite by a Serratia sp . from waste-water containing inorganic phosphate 3, 1723–1730.